Editors' Suggestion

Broadband Solenoidal Haloscope for Terahertz Axion Detection

Jesse Liu,[1,2,*] Kristin Dona,[2] Gabe Hoshino,[2,3] Stefan Knirck,[3,†] Noah Kurinsky,[3,4,5,‡] Matthew Malaker,[3] David W. Miller,[2,6,§] Andrew Sonnenschein,[3,‖] Mohamed H. Awida,[3] Peter S. Barry,[7,5] Karl K. Berggren,[8] Daniel Bowring,[3] Gianpaolo Carosi,[9] Clarence Chang,[7,5] Aaron Chou,[3] Rakshya Khatiwada,[3,10] Samantha Lewis,[3] Juliang Li,[7] Sae Woo Nam,[11] Omid Noroozian,[12] and Tony X. Zhou[8]

(BREAD Collaboration)

[1]*Cavendish Laboratory, University of Cambridge, Cambridge CB3 0HE, United Kingdom*
[2]*Department of Physics, University of Chicago, Chicago, Illinois 60637, USA*
[3]*Fermi National Accelerator Laboratory, Batavia, Illinois 60510, USA*
[4]*SLAC National Accelerator Laboratory, Menlo Park, California 94025, USA*
[5]*Kavli Institute for Cosmological Physics, University of Chicago, Chicago, Illinois 60637, USA*
[6]*Enrico Fermi Institute, University of Chicago, Chicago, Illinois 60637, USA*
[7]*Argonne National Laboratory, Lemont, Illinois 60439, USA*
[8]*Massachusetts Institute of Technology, Cambridge, Massachusetts 02139, USA*
[9]*Lawrence Livermore National Laboratory, Livermore, California 94551, USA*
[10]*Department of Physics, Illinois Institute of Technology, Chicago, Illinois 60616, USA*
[11]*National Institute of Standards and Technology, Boulder, Colorado 80305, USA*
[12]*NASA Goddard Space Flight Center, Greenbelt, Maryland 20771, USA*

(Received 25 November 2021; accepted 3 March 2022; published 28 March 2022)

We introduce the Broadband Reflector Experiment for Axion Detection (BREAD) conceptual design and science program. This haloscope plans to search for bosonic dark matter across the $[10^{-3}, 1]$ eV ([0.24, 240] THz) mass range. BREAD proposes a cylindrical metal barrel to convert dark matter into photons, which a novel parabolic reflector design focuses onto a photosensor. This unique geometry enables enclosure in standard cryostats and high-field solenoids, overcoming limitations of current dish antennas. A pilot 0.7 m^2 barrel experiment planned at Fermilab is projected to surpass existing dark photon coupling constraints by over a decade with one-day runtime. Axion sensitivity requires $< 10^{-20}$ W/$\sqrt{\text{Hz}}$ sensor noise equivalent power with a 10 T solenoid and 10 m^2 barrel. We project BREAD sensitivity for various sensor technologies and discuss future prospects.

DOI: 10.1103/PhysRevLett.128.131801

Introduction.—Astrophysical evidence for dark matter (DM) is unambiguous [1–6], but its particle properties remain enigmatic. Recent efforts are expanding bosonic DM searches for $m_{\text{DM}} \lesssim 1$ eV masses [7] predicted by many extensions of the standard model (SM) [8–14], complementing higher-mass searches [15–24]. Notably, the unobserved neutron electric dipole moment [25–28] motivates the quantum chromodynamics (QCD) axion a predicted by the Peccei-Quinn solution of the strong charge-parity problem [29–31]. Dark photons A' are also sought-after candidates arising in string theory scenarios [32–35]. These states have compelling early-Universe production mechanisms and their field oscillations with frequency $\nu = m_{\text{DM}}/2\pi$ exhibit DM properties [36–41]. Nonzero DM-photon couplings enable laboratory detection via electromagnetic (EM) effects.

The most-sensitive detection strategy today is the radio-frequency resonant-cavity haloscope [42–45], where ADMX [46–52], CAPP [53–55], HAYSTAC [56–59] probe QCD axions within $[1.8, 24]$ μeV masses. However, this strategy has long-standing obstacles from (i) narrow band tuning to unknown m_{DM} and (ii) impractical high-mass scaling for $m_{\text{DM}} \gtrsim 40$ μeV. Scan rates fall precipitously with photon frequency $R_{\text{scan}} \sim \nu^{-14/3}$ [59] and the number of required resonators scales unfavorably with effective volume $\sim m_{\text{DM}}^3$. Proposed dielectric haloscopes could probe $[40, 400]$ μeV [60–62] and [0.1, 10] eV [63] masses, while topological insulators target [0.7, 3.5] meV [64]. Significant sensitivity gaps persist across $[10^{-4}, 1]$ eV masses, favored by several theoretical scenarios [65–67], motivating broadband approaches.

This Letter introduces the Broadband Reflector Experiment for Axion Detection (BREAD) conceptual design to search multiple decades of DM mass without tuning to m_{DM}. BREAD proposes a novel experimental design that optimally realizes dish-antenna haloscopes [68].

Its hallmark is a cylindrical metal barrel for broadband DM-to-photon conversion with a coaxial parabolic reflector that focuses signal photons onto a sensor. In contrast to existing dish antennas using spherical or flat surfaces [69–73], our geometry is optimized for enclosure in standard cryostats and compact high-field solenoids. This enhances signal to noise, ensures the emitting surface and magnetic field are parallel, and keeps costs practical. We delineate the optical properties of this novel geometry with detailed ray tracing and numerical simulation. While photoconversion is broadband, photosensor performance governs final discovery reach. We assess various state-of-the-art sensors and discuss the advances required in quantum sensing technology for next-generation devices to fulfill BREAD science goals with broad anticipated impact in astronomy and beyond [74].

Dark matter signal.—Sub-eV-mass bosonic DM behave as classical fields, whose coherent oscillations generate the local halo energy density $\rho_{\rm DM}$, which we assume to be 0.45 GeV cm^{-3} [75]. We consider scenarios where either axions or dark photons exclusively saturate the halo DM. The DM-photon interaction augments the Ampère-Maxwell equation with an effective source current $\mathbf{J}_{\rm DM}$ [9]

$$\nabla \times \mathbf{B} - \partial_t \mathbf{E} = \mathbf{J}_{\rm DM}. \tag{1}$$

A nonzero $\mathbf{J}_{\rm DM}$ induces a small EM field that causes a discontinuity at the interface of media with different electric permittivity, such as a conducting dish in vacuum. To satisfy the $\mathbf{E}_\parallel = 0$ boundary condition parallel to the dish surface, a compensating EM wave with amplitude $|\mathbf{E}_0|$ must be emitted perpendicular to the surface. These waves transmit $P_{\rm DM} = \frac{1}{2}|\mathbf{E}_0|^2 A_{\rm dish}$ of power for dish area $A_{\rm dish}$. For axions with $g_{a\gamma\gamma}$ coupling to photons, the current is $\mathbf{J}_a = g_{a\gamma\gamma}\sqrt{2\rho_{\rm DM}}\mathbf{B}^{\parallel}_{\rm ext}\cos(m_a t)$ given an external magnetic field $\mathbf{B}^{\parallel}_{\rm ext}$ with nonzero component parallel to the plate, resulting in $P_a = \frac{1}{2}\rho_{\rm DM}(B^{\parallel}_{\rm ext} g_{a\gamma\gamma}/m_a)^2 A_{\rm dish}$ emitted power [68]. QCD axion models [80–84] relate $g_{a\gamma\gamma}$ to the mass by $g_{a\gamma\gamma} \sim 10^{-13}(m_a/\text{meV})$ GeV^{-1}, giving m_a-independent power. For dark photons with A'-SM kinetic mixing κ and polarization $\hat{\mathbf{n}}$, the current is $\mathbf{J}_{A'} = \kappa m_{A'}\sqrt{2\rho_{\rm DM}}\hat{\mathbf{n}}\cos(m_{A'}t)$, yielding $P_{A'} = \frac{1}{2}\rho_{\rm DM}\kappa^2 A_{\rm dish}\alpha^2_{\rm pol}$ power. The factor $\alpha_{\rm pol} = \sqrt{2/3}$ averages over A' polarizations [68]. $P_{A'}$ is $m_{A'}$-independent and persists even when $\mathbf{B}_{\rm ext} = \mathbf{0}$. Signal emission occurs independent of frequency in principle, allowing searches across several mass decades in single runs.

Practically, DM-detection sensitivity also depends on the signal emission-to-detection efficiency ϵ_s, photosensor noise equivalent power (NEP), and runtime Δt. NEP is defined as the incident signal power required to achieve unit signal-to-noise ratio (SNR) in a one Hertz bandwidth. We estimate sensitivity to $g_{a\gamma\gamma}$ and κ (squared) as the SNR exceeding five $\text{SNR} = (\epsilon_s P_{\rm DM}\sqrt{\Delta t})/\text{NEP} > 5$, where we assume sensors have sufficiently fast readout bandwidth $\mathcal{O}(100\ \text{kHz})$:

$$\left\{\begin{array}{l}\left(\frac{g_{a\gamma\gamma}}{10^{-11}}\right)^2\\ \left(\frac{\kappa}{10^{-14}}\right)^2\end{array}\right\} = \left\{\begin{array}{l}\frac{1.9}{\text{GeV}^2}\left(\frac{m_a}{\text{meV}}\frac{10\ \text{T}}{B_{\rm ext}}\right)^2\\ 7.6\frac{2/3}{\alpha^2_{\rm pol}}\end{array}\right\}\frac{10\ \text{m}^2}{A_{\rm dish}}\left(\frac{\text{hour}}{\Delta t}\right)^{1/2} \times \frac{\text{SNR}}{5}\frac{0.5}{\epsilon_s}\frac{\text{NEP}}{10^{-21}\ \text{W}/\sqrt{\text{Hz}}}\frac{0.45\ \text{GeV/cm}^3}{\rho_{\rm DM}}. \tag{2}$$

At high masses, shot noise is relevant due to insufficient signal photons $N_{\rm signal} = (\epsilon_s P_{\rm DM}\Delta t)/m_{\rm DM} < 5$. For the nominal $A_{\rm dish} = 10\ \text{m}^2$, $B_{\rm ext} = 10$ T configuration, QCD axions induce a few 1 eV photons week^{-1} so month-long runtimes render shot noise subdominant for $m_{\rm DM} \lesssim 1$ eV.

In photon-counting regimes, sensors with dark count rate DCR detect photons emitted at rate $R_{\rm DM} = P_{\rm DM}/m_{\rm DM}$. We use the counting-statistics significance $Z = N_{\rm signal}/\sqrt{N_{\rm noise}} = (\epsilon_s R_{\rm DM}\Delta t)/\sqrt{\text{DCR}\Delta t} > 5$ to estimate sensitivity in the background-limited regime. In the background-free photon-counting limit, the coupling sensitivity scales faster $g^{\rm sens}_{a\gamma\gamma} \propto (\Delta t)^{-1/2}$. With nominal photoconversion rates down to 1 photon per day, scaling as $R_\gamma \approx 10^{-5}(1\ \text{eV}/m_a)$ Hz, the photosensors considered are background limited. We thus constrain our projections to this scenario, where the Supplemental Material [85] discusses requirements of background-free experiments.

Coaxial haloscope design.—BREAD proposes a cylindrical barrel as the emitting surface and a novel reflector geometry comprising a coaxial parabolic surface of rotation around its tangent. This focuses the emitted radiation to a photosensor located on-axis at the parabola's vertex as shown in Fig. 1(a). DM-to-photon conversion also occurs at the parabolic surface but is not focused on the vertex. For a barrel with radius R and length $L = 2\sqrt{2}R$, the effective emitting area is $A_{\rm dish} = 2\pi RL$. This aspect ratio suits enclosure in conventional high-field solenoid magnets and ensures $\mathbf{B}_{\rm ext}$ is parallel to the emitting surface. Such magnets are widely used in basic or applied applications with fields reaching 10 T or higher [86,87].

While photoconversion occurs regardless of $m_{\rm DM}$, sensitivity is limited at high (low) masses by focusing (diffraction) effects. Both effects broaden the focal spot and reduce the geometric signal efficiency due to finite photosensor size. In the high-mass limit $\lambda_{\rm dB} \ll R$, DM-to-photon conversion occurs incoherently as the DM de Broglie wavelength $\lambda_{\rm dB}$ is smaller than the radius of the barrel $R \sim 1$ m. Here, the DM-halo velocity $v \simeq 10^{-3}$ smears out the focal spot size [88–90] on length scales larger than the signal-photon wavelength $\lambda_{\rm sig}$, rendering diffraction effects negligible. The blue line in Fig. 1(b) shows the expected intensity distribution at the focal spot for the most conservative case where the DM wind points along the least favorable direction. The gray line refers to a planar conversion surface of the same area comparable to other dish-antenna experiments [69–73] with an on-axis

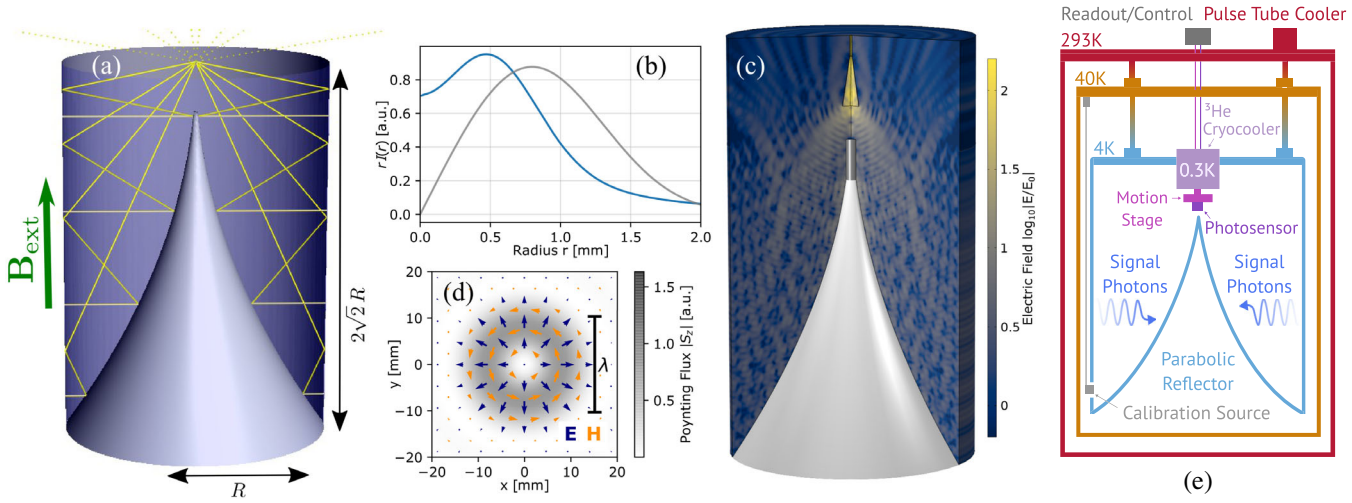

FIG. 1. (a) BREAD reflector geometry: rays (yellow lines) emitted from the cylindrical barrel, which is parallel to an external magnetic field $\mathbf{B}_{\text{ext}}$ from a surrounding solenoid (not shown) and focused at the vertex by a parabolic surface of revolution. (b) Radial intensity distribution $rI(r)$ expected from DM velocity effects in the xy plane at the focal spot using ray tracing, for the BREAD geometry as in (a) with $R = 20$ cm (blue) and for a conventional plane-parabolic mirror setup used in other experiments [69–73] with the same emitting surface area (gray). (c) Full field simulation at around 15 GHz including a preliminary coaxial horn design. (d) Electric (blue) and magnetic (orange) field distribution and time-averaged Poynting flux along the z direction in the xy plane at the focal spot. (e) Schematic setup in cryostat for pilot dark photon searches.

parabolic mirror at 1 m distance. Since rays impinge the focal plane from a larger solid angle, BREAD achieves improved focusing.

In the opposite low-mass limit $\lambda_{\text{dB}} \gg R$, such defocusing effects are negligible and the signal can be detected coherently. Figure 1(c) shows the result of a COMSOL simulation at around 15 GHz. Here the full modified Maxwell wave equation is solved to verify that there are no spurious sources or resonances excited that may interfere destructively with the signal. Figure 1(d) shows the diffraction-limited electromagnetic fields at the focal plane. The electric field polarized along the radial direction can be picked up by coaxial horn antennas [91,92]. Receiver designs based on microwave and submillimeter astronomy projects could be considered for signal collection. Proof-of-principle pilot experiments near both these limits are in preparation. The radio-frequency pilot targeting 10 s of GHz masses, called GigaBREAD, will be detailed in future work.

Figure 1(e) shows the proposed experimental design for the pilot A' search at infrared (IR) frequencies, called InfraBREAD. Cooling the conducting surfaces to 4 K suppresses thermal noise and we identified a large cryostat at Fermilab built to test ADMX resonators, which will be available in 2022. The barrel is constructed from aluminum with $A_{\text{dish}} = 0.7\ \text{m}^2 (10\ \text{m}^2)$ for the pilot (upgrade). A 4 K blackbody with $0.7\ \text{m}^2$ area and unit emissivity emits $\sim 10^{-8}$ W of power above 1 THz (4 meV). Simulation shows that thermal radiation is evenly distributed across the focal plane and so suppressed by $A_{\text{sens}}/A_{\text{dish}} \sim 10^{-6}$ for active sensor area A_{sens}. For $A_{\text{dish}} = 0.7\ \text{m}^2$, $A_{\text{sens}} = 0.5 \times 0.5\ \text{mm}^2$ yields 50% (25%) signal efficiency ϵ_s for optimistic (pessimistic) DM-wind alignment; see Supplemental Material [85] for further discussion. For absolute alignment of the photosensor in the reflector, we propose a piezoelectric motion stage to fine-tune the sensor position at the focus. Off focus, the signal is not enhanced. This enables *in situ* noise measurements by moving the single photosensor off axis or installing a second off-axis photosensor. A monochromatic laser or bandpass-filtered blackbody source can inject photons via a small hole in the barrel for absolute calibration of the reflector-photosensor setup. A room-temperature spectrometer at UChicago is available to characterize sources and filters [93].

Various upgrades and optimizations could be implemented to improve sensitivity of the proposed experimental concept. A small secondary mirror near the focal point could guide the signal toward a low-field region where, e.g., a chopper and/or spectrometer could be installed. The optics may optimize the radiation polarization and incident angle on the photosensors. A detector array or photon imager [94] could also provide spatial resolution to correlate any observed signals with the astrophysical DM distribution. Specifically, the focal point and signal undergo diurnal and annual modulations due to the rotating DM velocity vector in the lab frame [95] and possibly A' polarization [96]. The total A_{dish} could be increased within the same available volume by combining the signals from an array of smaller BREAD-like barrels, but this increases complexity significantly. Cosmic-ray muons are a suggested noise source for photon counters [97]; *in situ* vetoes at the sensor or barrel exterior, and/or underground operation are mitigation strategies. Studying these options is deferred to future work.

Photosensor technologies.—The expected DM signal rates and optical geometry imply stringent photosensor requirements: broad spectral response $\Delta E/E > 1$, ultralow noise NEP $< 10^{-20}$ W Hz$^{-1/2}$ or DCR $< 10^{-3}$ Hz, and millimeter-size active area. Bolometers are promising because they directly measure absorbed photon power, only the absorbing material or structures limit spectral response, and are established technology with diverse applications [98,99]. They comprise a thermally isolated absorbing element with low heat capacity, sensitive thermometer and weak link to a cold thermal bath. They can measure photon energies from 10^{-5} [100] to 10^{6} eV. Bolometers are typically insensitive to static (DC) radiation due to instrumental low-frequency ($1/f$) noise, so input signals must be time-modulated with, e.g., a chopper that shifts the signal to a frequency where $1/f$ noise is subdominant and SNR increases $\propto (\Delta t)^{1/2}$.

Photon-counting devices (photocounters) are potentially more sensitive than total-power bolometry, since simple signal-processing techniques, e.g., thresholding and pulse fitting, can suppress noise. Small devices achieve nearly background-free single-photon counting at thresholds $\gtrsim$1 eV. For lower energies, numerous devices exploit athermal breaking of Cooper pairs, including kinetic inductance detectors (KID), superconducting nanowire single photon detectors (SNSPD), and quantum capacitance detectors (QCDet) [101].

We now discuss specific technologies motivating the values in Table I assumed for our projections. We display typical $A_{\rm sens}$, but later set $\epsilon_s = 50\%$ for simplicity assuming sensor development will enable scaling to required sizes. Room-temperature (GENTEC pyroelectric [102]) and cryogenic (IR LABS semiconducting thermistor [103]) devices exemplify commercial performance.

Superconducting titanium-gold transition edge sensors (TES) [110–112] report down to 2×10^{-19} W Hz$^{-1/2}$ NEP in arrays of 200×200 μm^2 pixels [104]. TESs have broad spectral response, where a molybdenum-gold device reporting 4×10^{-19} W Hz$^{-1/2}$ NEP covers 1–4 μm to 160–960 μm (eV to meV) [113]. Elsewhere, small 10 μm superconducting–normal-metal junction bolometers report 2×10^{-20} W Hz$^{-1/2}$ NEP [114], which may be promising if active areas are scalable to millimeters [115].

KIDs [116–118] are thin-film resonators, whose surface inductance is sensitive to Cooper-pair-breaking photons above the band gap $\Delta \simeq 0.2$ meV. Titanium-nitride KIDs are scalable to 50×50 mm^2 kilopixel arrays with 3×10^{-19} W Hz$^{-1/2}$ NEP [105], which are antenna coupled and optimized to [3.4, 12] meV [119]. For cosmic microwave background (CMB) applications ($0.2 \lesssim E \lesssim 2$ meV), KIDs are limited by signal power rather than sensor noise at NEP $\sim 10^{-17}$ W Hz$^{-1/2}$ [120], and therefore could have better performance in such frequencies than current sensors targeting CMB science. Given KID and TES devices report similar NEP in each application, we amalgamate their presentation in our projections for simplicity. We extrapolate the 2×10^{-19} W Hz$^{-1/2}$ NEP [104] into the [0.2, 125] meV range where we expect KID/TES devices to operate bolometrically, but this will require experimental demonstration.

QCDets [121–123] recently report 3×10^{-21} W Hz$^{-1/2}$ NEP at 1.5 THz (6.2 meV) [106]. These are scalable to 441 pixel arrays and simulation indicates 1-4 $\times$ 10^{-20} W Hz$^{-1/2}$ NEP for [2, 125] meV [107], driven by, e.g., Origins Space Telescope goals [124]. Such performance is promising, and for simplicity, we assume constant 3×10^{-21} W Hz$^{-1/2}$ NEP in our projections. We convert this to DCR $= 4$ Hz using NEP $= (E/\eta)\sqrt{2 \cdot \text{DCR}}$ [125] for $E = 6.2$ meV and optical efficiency $\eta = 0.9$ [106].

SNSPDs [125–127] comprise sub-micron-width wires wound across thin-film substrates that count photons above an energy threshold. Superconductivity is momentarily lost upon photon absorption, leading to a measurable voltage pulse. Such devices achieve $> 90\%$ efficiency [128] and recently, a 400×400 μm^2 tungsten-silicide device reports DCR $< 10^{-4}$ Hz for 0.8 eV threshold [108]. Using Fermilab refrigerators [129], we are preparing to test similar SNSPDs fabricated at MIT. Recent advances important for BREAD include extending up to 10 μm (0.12 eV) [109] and developing large 3.1×3.1 mm^2 single pixels [130]. Continued research to lower thresholds is motivated given axions with $m_a \lesssim 60$ meV are disfavored by supernova constraints [131].

Photocounting is also possible using KIDs [132,133] and TESs [134–136], with the benefit of per-photon energy resolution. With, e.g., 10% energy resolution determined

TABLE I. Illustrative photosensor performance: spectral energy E, operating temperature $T_{\rm op}$, active area $A_{\rm sens}$. Bolometers (photocounters) report noise equivalent power NEP (dark count rate DCR).

Photosensor	(E/meV)	$(T_{\rm op}/\text{K})$	$[\text{NEP}/(\text{W}/\sqrt{\text{Hz}})]$	$(A_{\rm sens}/\text{mm}^2)$
GENTEC [102]	[0.4, 120]	293	1×10^{-8}	$\pi 2.5^2$
IR LABS [103]	[0.24, 248]	1.6	5×10^{-14}	1.5^2
KID/TES [104,105]	[0.2, 125]	0.3	2×10^{-19}	0.2^2
QCDet [106,107]	[2, 125]	0.015	$(\text{DCR}/\text{Hz}) = 4$	0.06^2
SNSPD [108,109]	[124, 830]	0.3	$(\text{DCR}/\text{Hz}) = 10^{-4}$	0.4^2

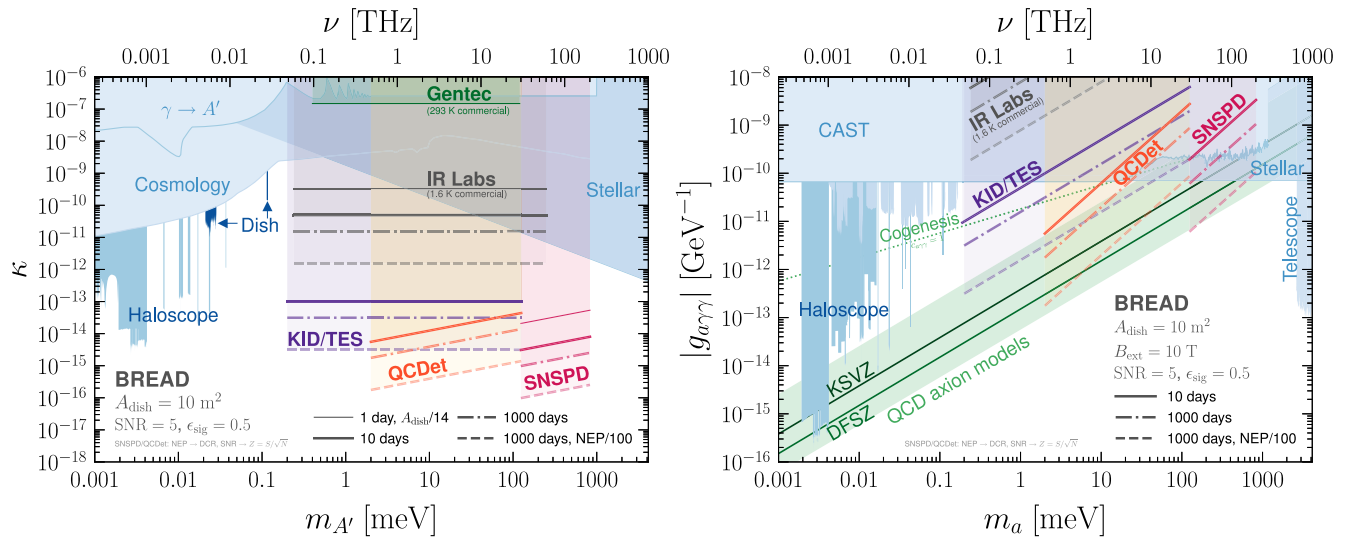

FIG. 2. Projected BREAD sensitivity by sensor technology (bold labels, see Table I) for dark photons A' (left) and axions a (right). This assumes signal-to-noise ratio SNR $= 5$ (significance $Z = 5$ for photocounters), signal efficiency $\epsilon_{\rm sig} = 0.5$, and dish area $A_{\rm dish} = 10$ m^2. Blue shading shows existing constraints from Ref. [96]. Benchmark axion predictions include QCD axion models [146] (green band), cogenesis [67] (green dots), KSVZ [82,83] and DFSZ [80,81] (green lines). Sensitivity scaling assumes background-limited operation where signal-power limits scale as $\sqrt{\Delta t}$ for runtime Δt and linearly with improved NEP.

by detector resolution, the monochromatic DM signal occupies one energy bin but noise can be spread across 10 bins, improving SNR after sufficient Δt up to a trials factor. Exploring this in BREAD requires more detailed resolution and noise models, which is deferred to future work.

Sensitivity and discussion.—We project BREAD sensitivity to dark photons in Fig. 2 (left) using Eq. (2) assuming the spectral and noise benchmarks in Table I. Existing constraints following Ref. [96] (blue shading) include stellar astrophysics [137,138], cosmology [40,139,140], and $\gamma \to A'$ conversion that includes laboratory probes [141,142]. With just 1 day runtime assuming $A_{\rm dish} = 0.7$ m^2, the gray thin line shows the BREAD pilot could surpass existing κ constraints by one decade around 1 meV using the commercial IR LABS sensor. The reach of BREAD is substantially broader compared with two existing dish antennas, SHUKET [143] and Tokyo [71] (dark blue). Importantly, BREAD probes higher masses than existing haloscopes ADMX [47,48], CAPP [53–55], HAYSTAC [58,59], transmon qubit [144], and WISPDMX [145], whose results are recasted for A' following Ref. [96]. Scaling to $A_{\rm dish} = 10$ m^2 and using KID/TES sensors could open two decades further κ sensitivity, while SNSPDs could achieve three decades gain for $m_{A'} \gtrsim 0.1$ eV. Extending runtime to $\Delta t = 10^3$ days enables κ sensitivity to reach six (four) decades beyond existing constraints for $m_{A'} \sim 0.4(200)$ meV.

Axion sensitivity is illustrated in Fig. 2 (right). Existing constraints [96] additionally include the CAST helioscope [147,148], telescopes [149,150], neutron stars [151–153], alongside ORGAN [154] QUAX [155,156] RADES [157] and URF [43–45] haloscopes. While challenging with commercial devices, 10 day runtimes using KID/TES sensors with NEP $\sim 10^{-19}$ W Hz$^{-1/2}$ could surpass CAST sensitivity for $m_a \lesssim 10$ meV. Longer runtimes could test cogenesis predictions for the $c_{a\gamma\gamma} = 1$ benchmark [67]. Increasing $A_{\rm dish}$ ($B_{\rm ext}$) beyond 10 m^2 (10 T) is financially unfavorable, requiring custom cryostats and magnets. Thus practically probing QCD axion models [146] requires longer runtime and lower sensor noise. Coupling sensitivity scales slowly with runtime $g^{\rm sens}_{a\gamma\gamma} \sim (\Delta t)^{-1/4}$, i.e., halving $g^{\rm sens}_{a\gamma\gamma}$ requires 16× longer runtimes. For $\Delta t = 10^3$ days, reaching KSVZ [82,83] (DFSZ [80,81]) demands $1(0.2) \times 10^{-22}$ W Hz$^{-1/2}$ NEP. Achieving this NEP for wide spectral ranges is challenging and a key science driver for sensor development. This may be attainable above 0.1 meV for photocounters, e.g., SNSPDs, motivating dedicated measurements in preparation, and next-generation bolometers at lower masses given a recent TES-based device reports 8×10^{-22} W Hz$^{-1/2}$ electrical NEP [158]. Maintaining signal efficiency when upgrading $A_{\rm dish} = 0.7 \to 10$ m^2 requires quadrupling the active sensor width. Overcoming these challenges promises significant scientific payoff given the multidecade improvements in search coverage that has long eluded cavity haloscopes. Post discovery, the DM signal will always persist, enabling cross checks with resonant techniques and measurements to elucidate its particle physics and astrophysical properties [70,96].

In summary, we proposed BREAD to improve sub-eV-mass DM reach by several decades. We introduced the novel coaxial design optimized for embedding in standard solenoids and cryostats, in contrast to existing dish antennas, then detailed numerical optics simulation and examined

photosensor candidates. Realizing BREAD into a cornerstone DM experiment will catalyze synergies across quantum technology and astroparticle physics.

We thank Ankur Agrawal, Israel Alatorre, Kate Azar, Lydia Beresford, Pierre Echternach, Juan Estrada, Amanda Farah, Casey Frantz, Mary Heintz, Chris Hill, Matthew Hollister, Reina Maruyama, Jan Offermann, Mark Oreglia, Jessica Schmidt, Sadie Seddon-Stettler, Danielle Speller, Emily Smith, Cecilia Tosciri, Liliana Valle, Joaquin Viera, and Steven Zoltowski for interesting and helpful discussions. This work is funded in part by the Department of Energy through the program for Quantum Information Science Enabled Discovery (QuantISED) for High Energy Physics and the resources of the Fermi National Accelerator Laboratory (Fermilab), a U.S. Department of Energy, Office of Science, HEP User Facility. Fermilab is managed by Fermi Research Alliance, LLC (FRA), acting under Contract No. DE-AC02-07CH11359. Work at Argonne National Laboratory is supported by the U.S. Department of Energy, Office of High Energy Physics, under Award No. DE-AC02-06CH11357. We acknowledge support by the Kavli Institute for Cosmological Physics at the University of Chicago through Grant No. NSF PHY-1125897 and an endowment from the Kavli Foundation and its founder Fred Kavli. Work at Lawrence Livermore National Laboratory is supported under Contract No. DE-AC52-07NA27344; Release No. LLNL-JRNL-828670. The MIT co-authors acknowledge support from the Fermi Research Alliance, LLC (FRA) and the US Department of Energy (DOE) under Contract No. DE-AC02-07CH11359. We thank the Aspen Center for Physics, which is supported by National Science Foundation Grant No. PHY-1607611, for hosting the Quantum Information Science for Fundamental Physics meeting (2020), and the University of Washington CENPA for the Axions Beyond Gen2 workshop (2021) supported by the Heising-Simons Foundation. J. L. acknowledges a University of Chicago fellowship supported by the Grainger Foundation, where this work began, and a Junior Research Fellowship at Trinity College, University of Cambridge.

*jesseliu@hep.phy.cam.ac.uk
†knirck@fnal.gov
‡kurinsky@slac.stanford.edu
§david.w.miller@uchicago.edu
‖sonnensn@fnal.gov

[1] V. C. Rubin and W. K. Ford, Jr., Rotation of the andromeda nebula from a spectroscopic survey of emission regions, Astrophys. J. **159**, 379 (1970).

[2] J. A. Tyson, G. P. Kochanski, and I. P. Dell'Antonio, Detailed mass map of CL0024 + 1654 from strong lensing, Astrophys. J. **498**, L107 (1998).

[3] M. Tegmark *et al.* (SDSS Collaboration), Cosmological parameters from SDSS and WMAP, Phys. Rev. D **69**, 103501 (2004).

[4] D. Clowe, M. Bradač, A. H. Gonzalez, M. Markevitch, S. W. Randall, C. Jones, and D. Zaritsky, A direct empirical proof of the existence of dark matter, Astrophys. J. **648**, L109 (2006).

[5] N. Aghanim *et al.* (Planck Collaboration), Planck 2018 results. I. Overview and the cosmological legacy of Planck, Astron. Astrophys. **641**, A1 (2020).

[6] G. Bertone, D. Hooper, and J. Silk, Particle dark matter: Evidence, candidates and constraints, Phys. Rep. **405**, 279 (2005).

[7] Natural units are used, where the (reduced) Planck's constant $\hbar$, speed of light c, vacuum permittivity ε_0 and permeability μ_0 are set to unity $\hbar = c = \varepsilon_0 = \mu_0 = 1$, as conventional in particle physics.

[8] A. Arvanitaki, S. Dimopoulos, S. Dubovsky, N. Kaloper, and J. March-Russell, String axiverse, Phys. Rev. D **81**, 123530 (2010).

[9] J. Jaeckel and A. Ringwald, The low-energy frontier of particle physics, Annu. Rev. Nucl. Part. Sci. **60**, 405 (2010).

[10] R. Essig *et al.*, Working group report: New light weakly coupled particles, in Community Summer Study 2013: Snowmass on the Mississippi (2013), arXiv:1311.0029.

[11] K. Baker *et al.*, The quest for axions and other new light particles, Ann. Phys. (Berlin) **525**, A93 (2013).

[12] M. Battaglieri *et al.*, New ideas in dark matter 2017: Community report, in U.S. Cosmic Visions (2017), arXiv:1707.04591.

[13] Z. Ahmed *et al.*, Quantum sensing for high energy physics, in First workshop on Quantum Sensing for High Energy Physics (2018), arXiv:1803.11306.

[14] I. G. Irastorza and J. Redondo, New experimental approaches in the search for axion-like particles, Prog. Part. Nucl. Phys. **102**, 89 (2018).

[15] D. S. Akerib *et al.* (LUX Collaboration), Results from a Search for Dark Matter in the Complete LUX Exposure, Phys. Rev. Lett. **118**, 021303 (2017).

[16] A. Tan *et al.* (PandaX-II Collaboration), Dark Matter Results from First 98.7 Days of Data from the PandaX-II Experiment, Phys. Rev. Lett. **117**, 121303 (2016).

[17] E. Aprile *et al.* (XENON Collaboration), Dark Matter Search Results from a One Ton-Year Exposure of XENON1T, Phys. Rev. Lett. **121**, 111302 (2018).

[18] R. Agnese *et al.* (SuperCDMS Collaboration), First Dark Matter Constraints from a SuperCDMS Single-Charge Sensitive Detector, Phys. Rev. Lett. **121**, 051301 (2018); **122**, 069901(E) (2019).

[19] A. Aguilar-Arevalo *et al.* (DAMIC Collaboration), Results on Low-Mass Weakly Interacting Massive Particles from an 11 kg d Target Exposure of DAMIC at SNOLAB, Phys. Rev. Lett. **125**, 241803 (2020).

[20] E. Izaguirre, G. Krnjaic, P. Schuster, and N. Toro, Analyzing the Discovery Potential for Light Dark Matter, Phys. Rev. Lett. **115**, 251301 (2015).

[21] A. Boveia and C. Doglioni, Dark matter searches at colliders, Annu. Rev. Nucl. Part. Sci. **68**, 429 (2018).

[22] ATLAS Collaboration, Searches for electroweak production of supersymmetric particles with compressed mass

spectra in $\sqrt{s} = 13$ TeV pp collisions with the ATLAS detector, Phys. Rev. D **101**, 052005 (2020).
[23] ATLAS Collaboration, Combination of Searches for Invisible Higgs Boson Decays with the ATLAS Experiment, Phys. Rev. Lett. **122**, 231801 (2019).
[24] ATLAS Collaboration, Search for new phenomena in events with an energetic jet and missing transverse momentum in pp collisions at $\sqrt{s} = 13$ TeV with the ATLAS detector, Phys. Rev. D **103**, 112006 (2021).
[25] P. G. Harris, C. A. Baker, K. Green, P. Iaydjiev, S. Ivanov, D. J. R. May, J. M. Pendlebury, D. Shiers, K. F. Smith, M. van der Grinten, and P. Geltenbort, New Experimental Limit on the Electric Dipole Moment of the Neutron, Phys. Rev. Lett. **82**, 904 (1999).
[26] C. A. Baker, D. D. Doyle, P. Geltenbort, K. Green, M. G. D. van der Grinten, P. G. Harris, P. Iaydjiev, S. N. Ivanov, D. J. R. May, J. M. Pendlebury, J. D. Richardson, D. Shiers, and K. F. Smith, Improved Experimental Limit on the Electric Dipole Moment of the Neutron, Phys. Rev. Lett. **97**, 131801 (2006).
[27] J. M. Pendlebury *et al.*, Revised experimental upper limit on the electric dipole moment of the neutron, Phys. Rev. D **92**, 092003 (2015).
[28] C. Abel *et al.* (nEDM Collaboration), Measurement of the Permanent Electric Dipole Moment of the Neutron, Phys. Rev. Lett. **124**, 081803 (2020).
[29] R. D. Peccei and H. R. Quinn, CP Conservation in the Presence of Instantons, Phys. Rev. Lett. **38**, 1440 (1977).
[30] F. Wilczek, Problem of Strong P and T Invariance in the Presence of Instantons, Phys. Rev. Lett. **40**, 279 (1978).
[31] S. Weinberg, A New Light Boson?, Phys. Rev. Lett. **40**, 223 (1978).
[32] B. Holdom, Two U(1)'s and epsilon charge shifts, Phys. Lett. **166B**, 196 (1986).
[33] K. R. Dienes, C. F. Kolda, and J. March-Russell, Kinetic mixing and the supersymmetric gauge hierarchy, Nucl. Phys. **B492**, 104 (1997).
[34] M. Pospelov, Secluded U(1) below the weak scale, Phys. Rev. D **80**, 095002 (2009).
[35] M. Goodsell, J. Jaeckel, J. Redondo, and A. Ringwald, Naturally light hidden photons in LARGE volume string compactifications, J. High Energy Phys. 11 (2009) 027.
[36] J. Preskill, M. B. Wise, and F. Wilczek, Cosmology of the invisible axion, Phys. Lett. **120B**, 127 (1983).
[37] L. F. Abbott and P. Sikivie, A cosmological bound on the invisible axion, Phys. Lett. **120B**, 133 (1983).
[38] M. Dine and W. Fischler, The not so harmless axion, Phys. Lett. **120B**, 137 (1983).
[39] A. E. Nelson and J. Scholtz, Dark light, dark matter and the misalignment mechanism, Phys. Rev. D **84**, 103501 (2011).
[40] P. Arias, D. Cadamuro, M. Goodsell, J. Jaeckel, J. Redondo, and A. Ringwald, WISPy cold dark matter, J. Cosmol. Astropart. Phys. 06 (2012) 013.
[41] F. Chadha-Day, J. Ellis, and D. J. E. Marsh, Axion dark matter: What is it and why now?, Sci. Adv. **8**, abj3618 (2022).
[42] P. Sikivie, Experimental Tests of the Invisible Axion, Phys. Rev. Lett. **51**, 1415 (1983); **52**, 695(E) (1984).
[43] S. DePanfilis, A. C. Melissinos, B. E. Moskowitz, J. T. Rogers, Y. K. Semertzidis, W. U. Wuensch, H. J. Halama, A. G. Prodell, W. B. Fowler, and F. A. Nezrick, Limits on the Abundance and Coupling of Cosmic Axions at $4.5 < m_a < 5.0$ μeV, Phys. Rev. Lett. **59**, 839 (1987).
[44] W. U. Wuensch, S. De Panfilis-Wuensch, Y. K. Semertzidis, J. T. Rogers, A. C. Melissinos, H. J. Halama, B. E. Moskowitz, A. G. Prodell, W. B. Fowler, and F. A. Nezrick, Results of a laboratory search for cosmic axions and other weakly coupled light particles, Phys. Rev. D **40**, 3153 (1989).
[45] C. Hagmann, P. Sikivie, N. S. Sullivan, and D. B. Tanner, Results from a search for cosmic axions, Phys. Rev. D **42**, 1297 (1990).
[46] S. Asztalos, E. Daw, H. Peng, L. J Rosenberg, C. Hagmann, D. Kinion, W. Stoeffl, K. van Bibber, P. Sikivie, N. S. Sullivan, D. B. Tanner, F. Nezrick, M. S. Turner, D. M. Moltz, J. Powell, M.-O. André, J. Clarke, M. Mück, and R. F. Bradley (ADMX Collaboration), Large scale microwave cavity search for dark matter axions, Phys. Rev. D **64**, 092003 (2001).
[47] S. J. Asztalos *et al.* (ADMX Collaboration), Experimental constraints on the axion dark matter halo density, Astrophys. J. Lett. **571**, L27 (2002).
[48] S. J. Asztalos, G. Carosi, C. Hagmann, D. Kinion, K. van Bibber, M. Hotz, L. J Rosenberg, G. Rybka, J. Hoskins, J. Hwang, P. Sikivie, D. B. Tanner, R. Bradley, and J. Clarke (ADMX Collaboration), SQUID-Based Microwave Cavity Search for Dark-Matter Axions, Phys. Rev. Lett. **104**, 041301 (2010).
[49] A. Wagner, G. Rybka, M. Hotz, L. J Rosenberg, S. J. Asztalos, G. Carosi, C. Hagmann, D. Kinion, K. van Bibber, J. Hoskins, C. Martin, P. Sikivie, D. B. Tanner, R. Bradley, and J. Clarke (ADMX Collaboration), A Search for Hidden Sector Photons with ADMX, Phys. Rev. Lett. **105**, 171801 (2010).
[50] N. Du *et al.* (ADMX Collaboration), A Search for Invisible Axion Dark Matter with the Axion Dark Matter Experiment, Phys. Rev. Lett. **120**, 151301 (2018).
[51] T. Braine *et al.* (ADMX Collaboration), Extended Search for the Invisible Axion with the Axion Dark Matter Experiment, Phys. Rev. Lett. **124**, 101303 (2020).
[52] C. Bartram *et al.* (ADMX Collaboration), Search for Invisible Axion Dark Matter in the $3.3 - 4.2$ μeV Mass Range, Phys. Rev. Lett. **127**, 261803 (2021).
[53] S. Lee, S. Ahn, J. Choi, B. R. Ko, and Y. K. Semertzidis, Axion Dark Matter Search around 6.7 μeV, Phys. Rev. Lett. **124**, 101802 (2020).
[54] J. Jeong, S. W. Youn, S. Bae, J. Kim, T. Seong, J. E. Kim, and Y. K. Semertzidis, Search for Invisible Axion Dark Matter with a Multiple-Cell Haloscope, Phys. Rev. Lett. **125**, 221302 (2020).
[55] O. Kwon *et al.* (CAPP Collaboration), First Results from an Axion Haloscope at CAPP around 10.7 μeV, Phys. Rev. Lett. **126**, 191802 (2021).
[56] S. Al Kenany *et al.*, Design and operational experience of a microwave cavity axion detector for the $20 - 100$ μeV range, Nucl. Instrum. Methods Phys. Res., Sect. A **854**, 11 (2017).
[57] B. M. Brubaker *et al.*, First Results from a Microwave Cavity Axion Search at 24 μeV, Phys. Rev. Lett. **118**, 061302 (2017).

[58] L. Zhong *et al.* (HAYSTAC Collaboration), Results from phase 1 of the HAYSTAC microwave cavity axion experiment, Phys. Rev. D **97**, 092001 (2018).
[59] K. M. Backes *et al.* (HAYSTAC Collaboration), A quantum-enhanced search for dark matter axions, Nature (London) **590**, 238 (2021).
[60] A. Caldwell, G. Dvali, B. Majorovits, A. Millar, G. Raffelt, J. Redondo, O. Reimann, F. Simon, and F. Steffen (MADMAX Collaboration), Dielectric Haloscopes: A New Way to Detect Axion Dark Matter, Phys. Rev. Lett. **118**, 091801 (2017).
[61] A. J. Millar, G. G. Raffelt, J. Redondo, and F. D. Steffen, Dielectric haloscopes to search for axion dark matter: Theoretical foundations, J. Cosmol. Astropart. Phys. 01 (2017) 061.
[62] P. Brun *et al.* (MADMAX Collaboration), A new experimental approach to probe QCD axion dark matter in the mass range above 40 μeV, Eur. Phys. J. C **79**, 186 (2019).
[63] M. Baryakhtar, J. Huang, and R. Lasenby, Axion and hidden photon dark matter detection with multilayer optical haloscopes, Phys. Rev. D **98**, 035006 (2018).
[64] D. J. E. Marsh, K.-C. Fong, E. W. Lentz, L. Smejkal, and M. N. Ali, Proposal to Detect Dark Matter using Axionic Topological Antiferromagnets, Phys. Rev. Lett. **123**, 121601 (2019).
[65] P. W. Graham, J. Mardon, and S. Rajendran, Vector dark matter from inflationary fluctuations, Phys. Rev. D **93**, 103520 (2016).
[66] M. Gorghetto, E. Hardy, and G. Villadoro, More axions from strings, SciPost Phys. **10**, 050 (2021).
[67] R. T. Co, L. J. Hall, and K. Harigaya, Predictions for axion couplings from ALP cogenesis, J. High Energy Phys. 01 (2021) 172.
[68] D. Horns, J. Jaeckel, A. Lindner, A. Lobanov, J. Redondo, and A. Ringwald, Searching for WISPy cold dark matter with a dish antenna, J. Cosmol. Astropart. Phys. 04 (2013) 016.
[69] J. Suzuki, T. Horie, Y. Inoue, and M. Minowa, Experimental search for hidden photon CDM in the eV mass range with a dish antenna, J. Cosmol. Astropart. Phys. 09 (2015) 042.
[70] S. Knirck, T. Yamazaki, Y. Okesaku, S. Asai, T. Idehara, and T. Inada, First results from a hidden photon dark matter search in the meV sector using a plane-parabolic mirror system, J. Cosmol. Astropart. Phys. 11 (2018) 031.
[71] N. Tomita, S. Oguri, Y. Inoue, M. Minowa, T. Nagasaki, J. Suzuki, and O. Tajima, Search for hidden-photon cold dark matter using a K-band cryogenic receiver, J. Cosmol. Astropart. Phys. 09 (2020) 012.
[72] A. Andrianavalomahefa, C. M. Schäfer, D. Veberič, R. Engel, T. Schwetz, H. J. Mathes, K. Daumiller, M. Roth, D. Schmidt, R. Ulrich, B. Döbrich, J. Jaeckel, M. Kowalski, A. Lindner, and J. Redondo (FUNK Experiment Collaboration), Limits from the funk experiment on the mixing strength of hidden-photon dark matter in the visible and near-ultraviolet wavelength range, Phys. Rev. D **102**, 042001 (2020).
[73] Brass website, http://wwwiexp.desy.de/groups/astroparticle/brass/brassweb.htm (accessed 2021-07-06).
[74] S. S. Dhillon, M. S. Vitiello, E. H. Linfield, A. G. Davies, M. C. Hoffmann, J. Booske, C. Paoloni, M. Gensch, P. Weightman, G. P. Williams *et al.*, The 2017 terahertz science and technology roadmap, J. Phys. D **50**, 043001 (2017).
[75] This value of ρ_{DM} is typically adopted in axion haloscope literature [50], but we note its significant uncertainties that range from $[0.2, 0.6]$ GeV cm^{-3} from global methods to $[0.4, 1.5]$ GeV cm^{-3} using recent astrometry data [76–79].
[76] J. I. Read, The local dark matter density, J. Phys. G **41**, 063101 (2014).
[77] M. Tanabashi *et al.* (Particle Data Group), Review of particle physics, Phys. Rev. D **98**, 030001 (2018).
[78] A. G. A. Brown *et al.* (Gaia Collaboration), Gaia Data Release 2: Summary of the contents and survey properties, Astron. Astrophys. **616**, A1 (2018).
[79] J. Buch, S. C. Leung, and J. Fan, Using Gaia DR2 to constrain local dark matter density and thin dark disk, J. Cosmol. Astropart. Phys. 04 (2019) 026.
[80] M. Dine, W. Fischler, and M. Srednicki, A simple solution to the strong CP problem with a harmless axion, Phys. Lett. **104B**, 199 (1981).
[81] A. R. Zhitnitsky, On possible suppression of the axion hadron interactions. (In Russian), Sov. J. Nucl. Phys. **31**, 260 (1980).
[82] J. E. Kim, Weak Interaction Singlet and Strong CP Invariance, Phys. Rev. Lett. **43**, 103 (1979).
[83] M. A. Shifman, A. I. Vainshtein, and V. I. Zakharov, Can confinement ensure natural CP invariance of strong interactions? Nucl. Phys. **B166**, 493 (1980).
[84] G. Grilli di Cortona, E. Hardy, J. Pardo Vega, and G. Villadoro, The QCD axion, precisely, J. High Energy Phys. 01 (2016) 034.
[85] See Supplemental Material at http://link.aps.org/supplemental/10.1103/PhysRevLett.128.131801 for additional information on axion and dark photon single rate, cryostat and magnet considerations, dark matter velocity effects, photosensor performance and noise sources, and experimental staging.
[86] T. F. Budinger and M. D. Bird, MRI and MRS of the human brain at magnetic fields of 14 T to 20 T: Technical feasibility, safety, and neuroscience horizons, NeuroImage **168**, 509 (2018).
[87] M. D. Bird, Ultra-high field solenoids and axion detection, Springer Proc. Phys. **245**, 9 (2020).
[88] J. Jaeckel and J. Redondo, An antenna for directional detection of WISPy dark matter, J. Cosmol. Astropart. Phys. 11 (2013) 016.
[89] J. Jaeckel and S. Knirck, Directional resolution of dish antenna experiments to search for WISPy dark matter, J. Cosmol. Astropart. Phys. 01 (2016) 005.
[90] J. Jaeckel and S. Knirck, Dish antenna searches for WISPy dark matter: Directional resolution small mass limitations, in *Proceedings of the 12th Patras Workshop on Axions, WIMPs and WISPs (PATRAS 2016): Jeju Island, South Korea, 2016* (2017), pp. 78–81, 10.3204/DESY-PROC-2009-03/Knirck_Stefan.
[91] F. J. B. Barros, S. P. Silva, W. S. Fonseca, S. R. Zang, and J. R. Bergmann, Analysis of a coaxial horn antenna using FDTD bidimensional method, in *Proceedings of the 2013 SBMO/IEEE MTT-S International Microwave Optoelectronics Conference (IMOC)* (2013), pp. 1–4, 10.1109/IMOC.2013.6646569.
[92] D. N. Bykov, N. M. Bykov, A. I. Klimov, I. K. Kurkan, and V. V. Rostov, A wideband converter of the main mode of

the coaxial line into the lowest symmetric mode of a circular waveguide, Instrum. Exp. Tech. **51**, 724 (2008).
[93] K. Dona, J. Liu, N. Kurinsky, D. Miller, P. Barry, C. Chang, and A. Sonnenschein, Design and performance of a multi-terahertz Fourier transform spectrometer for axion dark matter experiments, arXiv:2104.07157.
[94] Q. Zhao, D. Zhu, N. Calandri, A. Dane, A. McCaughan, F. Bellei, H.-Z. Wang, D. Santavicca, and K. Berggren, Single-photon imager based on a superconducting nanowire delay line, Nat. Photonics **11**, 247 (2017).
[95] S. Knirck, A. J. Millar, C. A. J. O'Hare, J. Redondo, and F. D. Steffen, Directional axion detection, J. Cosmol. Astropart. Phys. 11 (2018) 051.
[96] A. Caputo, A. J. Millar, C. A. J. O'Hare, and E. Vitagliano, Dark photon limits: A handbook, Phys. Rev. D **104**, 095029 (2021).
[97] J. Allmaras, K. Berggren, I. Charaev, C. Chang, J. Chiles, B. Korzh, A. Lita, J. Luskin, S. W. Nam, V. Novosad, M. Shaw, V. Verma, and E. Wollman, *Superconducting Nanowire Single-Photon Detectors* (2020), SNOWMASS21-IF1-IF2-CF1-CF0-147, https://www.snowmass21.org/docs/files/summaries/IF/SNOWMASS21-IF1_IF2-CF1_CF0-147.pdf.
[98] P. L. Richards, Bolometers for infrared and millimeter waves, J. Appl. Phys. **76**, 1 (1994).
[99] S. Pirro and P. Mauskopf, Advances in bolometer technology for fundamental physics, Annu. Rev. Nucl. Part. Sci. **67**, 161 (2017).
[100] R. Kokkoniemi *et al.*, Bolometer operating at the threshold for circuit quantum electrodynamics, Nature (London) **586**, 47 (2020).
[101] QCDet representing quantum capacitance detector avoids ambiguity with QCD denoting quantum chromodynamics.
[102] Gentec Electro-Optics, https://www.gentec-eo.com/products/thz5b-bl-da-d0.
[103] Infrared Laboratories, Bolometers.
[104] M. L. Ridder, P. Khosropanah, R. A. Hijmering, T. Suzuki, M. P. Bruijn, H. F. C. Hoevers, J. R. Gao, and M. R. Zuiddam, Fabrication of low-noise TES arrays for the SAFARI instrument on SPICA, J. Low Temp. Phys. **184**, 60 (2016).
[105] J. J. A. Baselmans *et al.*, A kilo-pixel imaging system for future space based far-infrared observatories using microwave kinetic inductance detectors, Astron. Astrophys. **601**, A89 (2017).
[106] P. M. Echternach, B. J. Pepper, T. Reck, and C. M. Bradford, Single photon detection of 1.5 THz radiation with the quantum capacitance detector, Nat. Astron. **2**, 90 (2018).
[107] P. M. Echternach, A. D. Beyer, and C. M. Bradford, Large array of low-frequency readout quantum capacitance detectors, J. Astron. Telesc. Instrum. Syst. **7**, 1 (2021).
[108] Y. Hochberg, I. Charaev, S.-W. Nam, V. Verma, M. Colangelo, and K. K. Berggren, Detecting Sub-GeV Dark Matter with Superconducting Nanowires, Phys. Rev. Lett. **123**, 151802 (2019).
[109] V. B. Verma *et al.*, Single-photon detection in the mid-infrared up to 10 micron wavelength using tungsten silicide superconducting nanowire detectors, arXiv:2012.09979.
[110] K. D. Irwin, An application of electrothermal feedback for high resolution cryogenic particle detection, Appl. Phys. Lett. **66**, 1998 (1995).
[111] K. D. Irwin and G. C. Hilton, Transition-edge sensors, in *Cryogenic Particle Detection* (Springer, New York), pp. 63–150.
[112] T. Gerrits, A. Lita, B. Calkins, and S. W. Nam, Superconducting transition edge sensors for quantum optics, in *Superconducting Devices in Quantum Optics. Quantum Science and Technology* (Springer, New York, 2016).
[113] D. J. Goldie, A. V. Velichko, D. M. Glowacka, and S. Withington, Ultra-low-noise MoCu transition edge sensors for space applications, J. Appl. Phys. **109**, 084507 (2011).
[114] R. Kokkoniemi *et al.*, Nanobolometer with ultralow noise equivalent power, Commun. Phys. **2**, 124 (2019).
[115] X. Zhang, I. Charaev, H. Liu, T. X. Zhou, D. Zhu, K. K. Berggren, and A. Schilling, Physical properties of amorphous molybdenum silicide films for single-photon detectors, Supercond. Sci. Technol. **34**, 095003 (2021).
[116] P. K. Day, H. G. LeDuc, B. A. Mazin, A. Vayonakis, and J. Zmuidzinas, A broadband superconducting detector suitable for use in large arrays, Nature (London) **425**, 817 (2003).
[117] H. G. Leduc, B. Bumble, P. K. Day, B. H. Eom, J. Gao, S. Golwala, B. A. Mazin, S. McHugh, A. Merrill, D. C. Moore, O. Noroozian, A. D. Turner, and J. Zmuidzinas, Titanium nitride films for ultrasensitive microresonator detectors, Appl. Phys. Lett. **97**, 102509 (2010).
[118] J. Zmuidzinas, Superconducting microresonators: Physics and applications, Annu. Rev. Condens. Matter Phys. **3**, 169 (2012).
[119] B. D. Jackson *et al.*, The SPICA-SAFARI detector system: TES detector arrays with frequency-division multiplexed SQUID readout, IEEE Trans. Terahertz Sci. Technol. **2**, 12 (2012).
[120] M. H Abitbol *et al.*, CMB-S4 technology book, arXiv:1706.02464.
[121] M. D. Shaw, J. Bueno, P. Day, C. M. Bradford, and P. M. Echternach, Quantum capacitance detector: A pair-breaking radiation detector based on the single cooper-pair box, Phys. Rev. B **79**, 144511 (2009).
[122] J. Bueno, M. D. Shaw, P. K. Day, and P. M. Echternach, Proof of concept of the quantum capacitance detector, Appl. Phys. Lett. **96**, 103503 (2010).
[123] P. M. Echternach, K. J. Stone, C. M. Bradford, P. K. Day, D. W. Wilson, K. G. Megerian, N. Llombart, and J. Bueno, Photon shot noise limited detection of terahertz radiation using a quantum capacitance detector, Appl. Phys. Lett. **103**, 053510 (2013).
[124] D. T. Leisawitz *et al.*, Origins space telescope: Baseline mission concept, J. Astron. Telesc. Instrum. Syst. **7**, 1 (2021).
[125] L. Chen, D. Schwarzer, J. A. Lau, V. B. Verma, M. J. Stevens, F. Marsili, R. P. Mirin, S. W. Nam, and A. M. Wodtke, Ultra-sensitive mid-infrared emission spectrometer with sub-ns temporal resolution, Opt. Express **26**, 14859 (2018).
[126] G. N. Gol'tsman, O. Okunev, G. Chulkova, A. Lipatov, A. Semenov, K. Smirnov, B. Voronov, A. Dzardanov, G. Williams, and R. Sobolewski, Picosecond superconducting single photon optical detector, Appl. Phys. Lett. **79**, 705 (2001).

[127] C. M. Natarajan, M. G. Tanner, and R. H. Hadfield, Superconducting nanowire single-photon detectors: Physics and applications, Supercond. Sci. Technol. **25**, 063001 (2012).

[128] F. Marsili, V. B. Verma, J. A. Stern, S. Harrington, A. E. Lita, T. Gerrits, I. Vayshenker, B. Baek, M. D. Shaw, R. P. Mirin, and S. W. Nam, Detecting single infrared photons with 93% system efficiency, Nat. Photonics **7**, 210 (2013).

[129] I. Hernandez, G. Cancelo, J. Estrada, H. Gonzalez, A. Lathrop, M. Makler, and C. Stoughto, Interplay between phonon downconversion efficiency, density of states at Fermi energy, and intrinsic energy resolution for microwave kinectic inductance detectors, arXiv:2004.04266.

[130] E. E. Wollman *et al.*, Recent advances in superconducting nanowire single-photon detector technology for exoplanet transit spectroscopy in the mid-infrared, J. Astron. Telesc. Instrum. Syst. **7**, 1 (2021).

[131] J. H. Chang, R. Essig, and S. D. McDermott, Supernova 1987A constraints on sub-GeV dark sectors, millicharged particles, the QCD axion, and an axion-like particle, J. High Energy Phys. 09 (2018) 051.

[132] J. Gao *et al.*, A titanium-nitride near-infrared kinetic inductance photon-counting detector and its anomalous electrodynamics, Appl. Phys. Lett. **101**, 142602 (2012).

[133] P. J. de Visser, S. A. H. de Rooij, V. Murugesan, D. J. Thoen, and J. J. A. Baselmans, Phonon-trapping enhanced energy resolution in superconducting single photon detectors, Phys. Rev. Applied **16**, 034051 (2021).

[134] A. Miller, S. W. Nam, J. Martinis, and A. Sergienko, Demonstration of a low-noise near-infrared photon counter with multiphoton discrimination, Appl. Phys. Lett. **83**, 791 (2003).

[135] A. E. Lita, A. J. Miller, and S. W. Nam, Counting near-infrared single-photons with 95% efficiency, Opt. Express **16**, 3032 (2008).

[136] B. S. Karasik, S. V. Pereverzev, A. Soibel, D. F. Santavicca, D. E. Prober, D. Olaya, and M. E. Gershenson, Energy-resolved detection of single infrared photons with $\lambda = 8$ μm using a superconducting microbolometer, Appl. Phys. Lett. **101**, 052601 (2012).

[137] J. Redondo and G. Raffelt, Solar constraints on hidden photons re-visited, J. Cosmol. Astropart. Phys. 08 (2013) 034.

[138] N. Vinyoles, A. Serenelli, F. L. Villante, S. Basu, J. Redondo, and J. Isern, New axion and hidden photon constraints from a solar data global fit, J. Cosmol. Astropart. Phys. 10 (2015) 015.

[139] S. D. McDermott and S. J. Witte, Cosmological evolution of light dark photon dark matter, Phys. Rev. D **101**, 063030 (2020).

[140] A. Caputo, H. Liu, S. Mishra-Sharma, and J. T. Ruderman, Dark Photon Oscillations in Our Inhomogeneous Universe, Phys. Rev. Lett. **125**, 221303 (2020).

[141] M. Betz, F. Caspers, M. Gasior, M. Thumm, and S. W. Rieger, First results of the CERN Resonant Weakly Interacting sub-eV Particle Search (CROWS), Phys. Rev. D **88**, 075014 (2013).

[142] D. Kroff and P. C. Malta, Constraining hidden photons via atomic force microscope measurements and the Plimpton-Lawton experiment, Phys. Rev. D **102**, 095015 (2020).

[143] P. Brun, L. Chevalier, and C. Flouzat, Direct Searches for Hidden-Photon Dark Matter with the SHUKET Experiment, Phys. Rev. Lett. **122**, 201801 (2019).

[144] A. V. Dixit, S. Chakram, K. He, A. Agrawal, R. K. Naik, D. I. Schuster, and A. Chou, Searching for Dark Matter with a Superconducting Qubit, Phys. Rev. Lett. **126**, 141302 (2021).

[145] L. H. Nguyen, A. Lobanov, and D. Horns, First results from the WISPDMX radio frequency cavity searches for hidden photon dark matter, J. Cosmol. Astropart. Phys. 10 (2019) 014.

[146] L. Di Luzio, F. Mescia, and E. Nardi, Redefining the Axion Window, Phys. Rev. Lett. **118**, 031801 (2017).

[147] M. Arik *et al.* (CAST Collaboration), Search for Solar Axions by the CERN Axion Solar Telescope with ^{3}He Buffer Gas: Closing the Hot Dark Matter Gap, Phys. Rev. Lett. **112**, 091302 (2014).

[148] V. Anastassopoulos *et al.* (CAST Collaboration), New CAST limit on the axion-photon interaction, Nat. Phys. **13**, 584 (2017).

[149] D. Grin, G. Covone, J.-P. Kneib, M. Kamionkowski, A. Blain, and E. Jullo, A Telescope Search for Decaying Relic Axions, Phys. Rev. D **75**, 105018 (2007).

[150] M. Regis, M. Taoso, D. Vaz, J. Brinchmann, S. L. Zoutendijk, N. F. Bouché, and M. Steinmetz, Searching for light in the darkness: Bounds on ALP dark matter with the optical MUSE-faint survey, Phys. Lett. B **814**, 136075 (2021).

[151] J. W. Foster, Y. Kahn, O. Macias, Z. Sun, R. P. Eatough, V. I. Kondratiev, W. M. Peters, C. Weniger, and B. R. Safdi, Green Bank and Effelsberg Radio Telescope Searches for Axion Dark Matter Conversion in Neutron Star Magnetospheres, Phys. Rev. Lett. **125**, 171301 (2020).

[152] J. Darling, New limits on axionic dark matter from the magnetar PSR J1745-2900, Astrophys. J. Lett. **900**, L28 (2020).

[153] R. A. Battye, J. Darling, J. I. McDonald, and S. Srinivasan, Towards robust constraints on axion dark matter using PSR J1745-2900, Phys. Rev. D **105**, L021305 (2022).

[154] B. T. McAllister, G. Flower, E. N. Ivanov, M. Goryachev, J. Bourhill, and M. E. Tobar, The ORGAN experiment: An axion haloscope above 15 GHz, Phys. Dark Universe **18**, 67 (2017).

[155] D. Alesini *et al.*, Galactic axions search with a superconducting resonant cavity, Phys. Rev. D **99**, 101101(R) (2019).

[156] D. Alesini *et al.*, Search for invisible axion dark matter of mass $m_a = 43$ μeV with the QUAX–$a\gamma$ experiment, Phys. Rev. D **103**, 102004 (2021).

[157] A. Álvarez Melcón *et al.* (CAST Collaboration), First results of the CAST-RADES haloscope search for axions at 34.67 μeV, J. High Energy Phys. 10 (2021) 075.

[158] P. C. Nagler, J. E. Sadleir, and E. J. Wollack, Demonstration of ultra-low noise equivalent power using a longitudinal proximity effect transition-edge sensor, arXiv:2012.06543.